



Ricerca di Sistema elettrico

Analisi preliminare dei materiali alternativi per la realizzazione del target assembly di IFMIF

Luciano Pilloni, Carlo Cristalli

ANALISI PRELIMINARE DEI MATERIALI ALTERNATIVI PER LA REALIZZAZIONE DEL TARGET ASSEMBLY DI IFMIF

Luciano Pilloni, Carlo Cristalli (ENEA)

Settembre 2014

Report Ricerca di Sistema Elettrico

Accordo di Programma Ministero dello Sviluppo Economico – ENEA

Piano Annuale di Realizzazione 2013

Area: Produzione di Energia Elettrica e Protezione dell'Ambiente

Progetto: Attività di fisica della Fusione complementari a ITER

Obiettivo: Forniture ed implementazioni comuni per progettazione completa di target assembly per IFMIF

Responsabile del Progetto: Aldo Pizzuto, ENEA

Index

SUMMARY	4
1 INTRODUCTION.....	5
2 DESCRIPTION OF ACTIVITIES AND RESULTS	15
2.1 THERMODYNAMIC SIMULATIONS.....	15
2.2 FABBRICATION	22
2.3 FABBRICAZIONE LINGOTTO 7Cr (MINI REPORT CSM)	22
3 CONCLUSIONI.....	25
4 RIFERIMENTI BIBLIOGRAFICI.....	25
5 ABBREVIAZIONI ED ACRONIMI.....	26

Summary

In this short summary we report the activity carried out in the frame of PAR for Fusion 2013-2014.

The aim of these activities was to design and to produce a small cast of reduced activation martensitic steel for Fusion applications, fabricated by Centro Sviluppo Materiali (CSM), Via di Castel Romano, Roma

The results of European studies on Fusion martensitic alloys, which identified the EUROFER 97 as reference alloy for fusion application, showed that the principal limitation in the use of this alloy is the embrittlement due to neutron irradiation at temperature lower than about 380°C. This behaviour is due primary to the interstitial loops generated by irradiation that, under about 400°C, harden the matrix, conducting the alloy to have a brittle behaviour (fig.1a).

This fact is common to all alloys developed for fusion applications (9Cr2WVA ORNL, F82H ecc.) and is well documented in the literature [1].

The recent EUROFUSION requirements indicate that the first DEMO reactor will be water -cooled. This implies that the minimum irradiation temperature would be about 280°C. So, in the WP-MAT, in light of the under irradiation behaviour of EUROFER, it was decided to develop a much tough alloy, able to tolerate the so low irradiation temperature.

The guidelines we used to obtain this requirement are illustrated in the following:

- To Reduce the chromium amount compatibly with corrosion behaviour and in the range of RAFM just studied (e.g. F82H);
- To Reduce of Nitrogen content to have a slightly soft matrix and to reduce secondary precipitation at the tempering temperature (VTaN)
- To reduce the Vanadium amount for the same reasons.
- To keep the Ta and Carbon concentrations at the same value of Eurofer to have the primary precipitation required to refine the grain size.
- To study the effect of multi-austenitization treatments before tempering in order to have at the same time small grain size and finer primary precipitation of TaC and to fix, after investigations, the normalizing and tempering treatment.

After several thermodynamic simulations with the software Thermocalc (Fig.2), we have fixed the chemical composition and specification that was given to CSM (table 1) to fabricate the cast. The cast was recently fabricated. The heat treatments investigations and microstructural and mechanical characterizations will be the object of future investigations.

1 Introduction

The results of European effort to define a Reduced Activation Ferritic Martensitic steel (RAFM) brought to define the EUROFER97 steel, fabricated in an sufficiently high amount, by Boheler. In the following we report out of pile mechanical and microstructural characteristics taken from the report FZK[] and the after irradiation behaviour

The chemical composition (specifications) of EUROFER 97 is reported in the following table

Table 1. Chemical specification of EUROFER 97

	Element	Minimum Value (wt. %)	Maximum Value (wt. %)	Remarks/Target
A)	Cr	8.50	9.50	9.0
	C	0.090	0.120	0.11
	Mn	0.20	0.60	0.4
	P		0.005	
	S		0.005	
	V	0.15	0.25	
	B		0.001	ALAP
	N ₂	0.015	0.045	0.03
	O ₂		0.01	
B)	W	1.0	1.2	
	Ta	0.05	0.09	
	Ti		0.01	
C)	Nb		0.001	ALAP
	Mo		0.005	ALAP
	Ni		0.005	ALAP
	Cu		0.005	ALAP
	Al		0.01	ALAP
	Si		0.050	
	Co		0.005	ALAP
	As+Sn+Sb+Zr		0.05	

A) basic composition

B) varied substitution elements

C) radiological undesirable tramp elements

ALAP = as low as possible

Table 2. Chemical composition of heat 83699/83698 measured by different laboratory

	Specification	A Producer analysis heat 83699/83698 (Ø100 mm/ 14 mm)	B IMF analysis heat 83698 1.5 mm plate	C CEA analysis 3 heats 5 sizes (see [51])
Cr	8.50-9.50 %	8.87/8.82 %	9.21 %	8.68-9.04 %
C	0.09-0.12	0.12/0.11	0.104	0.092-0.117
Mn	0.20-0.60	0.42/0.47	0.502	0.41-0.50
V	0.15-0.25	0.19/0.20	0.204	0.17-0.19
W	1.0-1.2	1.10/1.09	1.148	1.03-1.26
Ta	0.05-0.09	0.14/0.13	0.14	0.10-0.15
N ₂	0.015-0.045	0.018/0.020	0.0234	0.018-0.0226
O ₂	max. 0.01	0.0013/0.0010	<0.001	0.0005-0.0011
P	max. 0.005	0.004/0.005	<0.04	0.011-0.013
S	max. 0.005	0.003/0.004	0.004	<0.003
B	max. 0.001 ¹⁾	<0.0005/0.001	<0.01	<0.001
Ti	max. 0.01	0.008/0.005	0.004	0.001-0.005
Nb	max. 0.001 ¹⁾	<0.0010/0.0016	12 ppm	<20 ppm
Mo	max. 0.005 ¹⁾	<0.0010/0.0010	<8	<20-100
Ni	max. 0.005 ¹⁾	<0.007/0.0200	214	400-600
Cu	max. 0.005 ¹⁾	0.022/0.0016	35	30-400
Al	max. 0.01 ¹⁾	0.008/0.009	51	30-40
Si	max. 0.05 ¹⁾	0.07/0.04	430	300-600
Co	max. 0.005 ¹⁾	0.004/0.006	67	80-200
As+Sn+Sb+Zr	max. 0.05	<0.015/0.015		<65-145

¹⁾ ALAP (as low as possible)

Carbon and Tantalum are slightly out of specifications.

Several heat treatments of austenitizing and tempering were experimented on this alloy. We report in the following figure relating the austenitization treatment to the Prior Austenite Grain Size (PAGs).

In that follows we show the mechanical characteristics as a function of heat treatment.

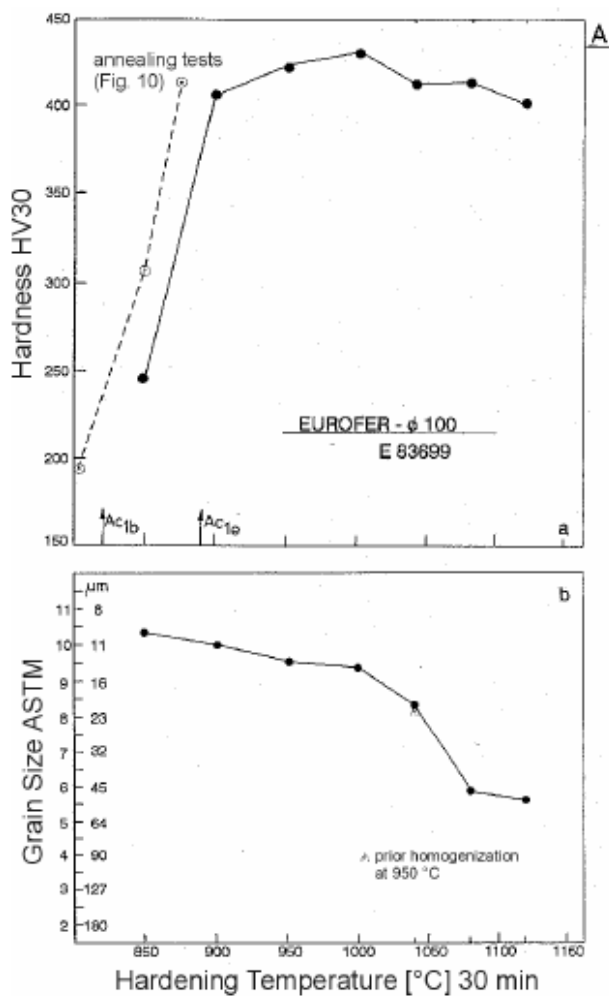


Fig.1 - Effect of austenitizing temperature (30') on grain size (PAG)

As the figure show, the lower the temperature the lower grain size and this fact could have a relevant effect on fracture toughness.

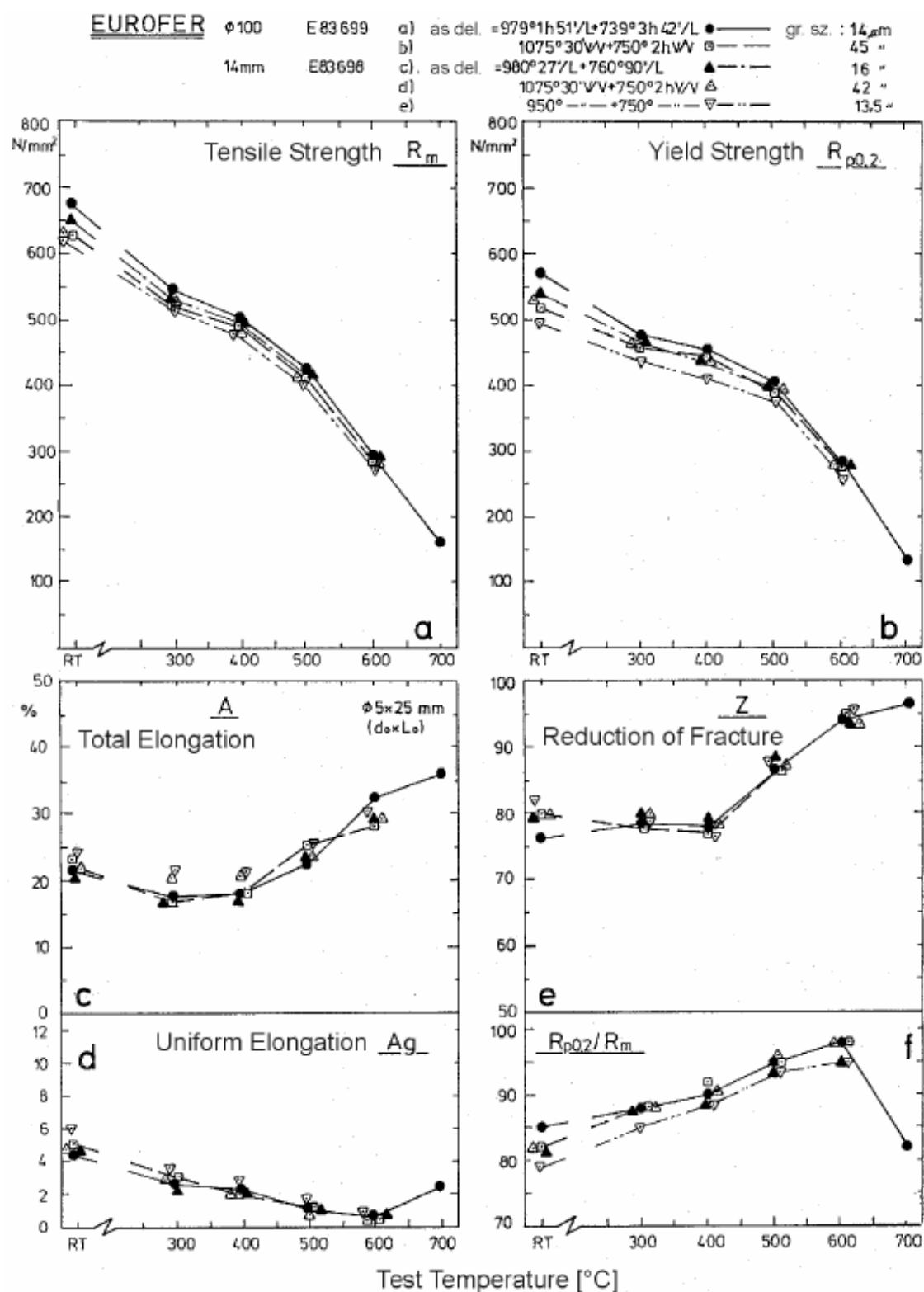


Fig.2 – Tensile test values as a function of test temperature for different heat treatment

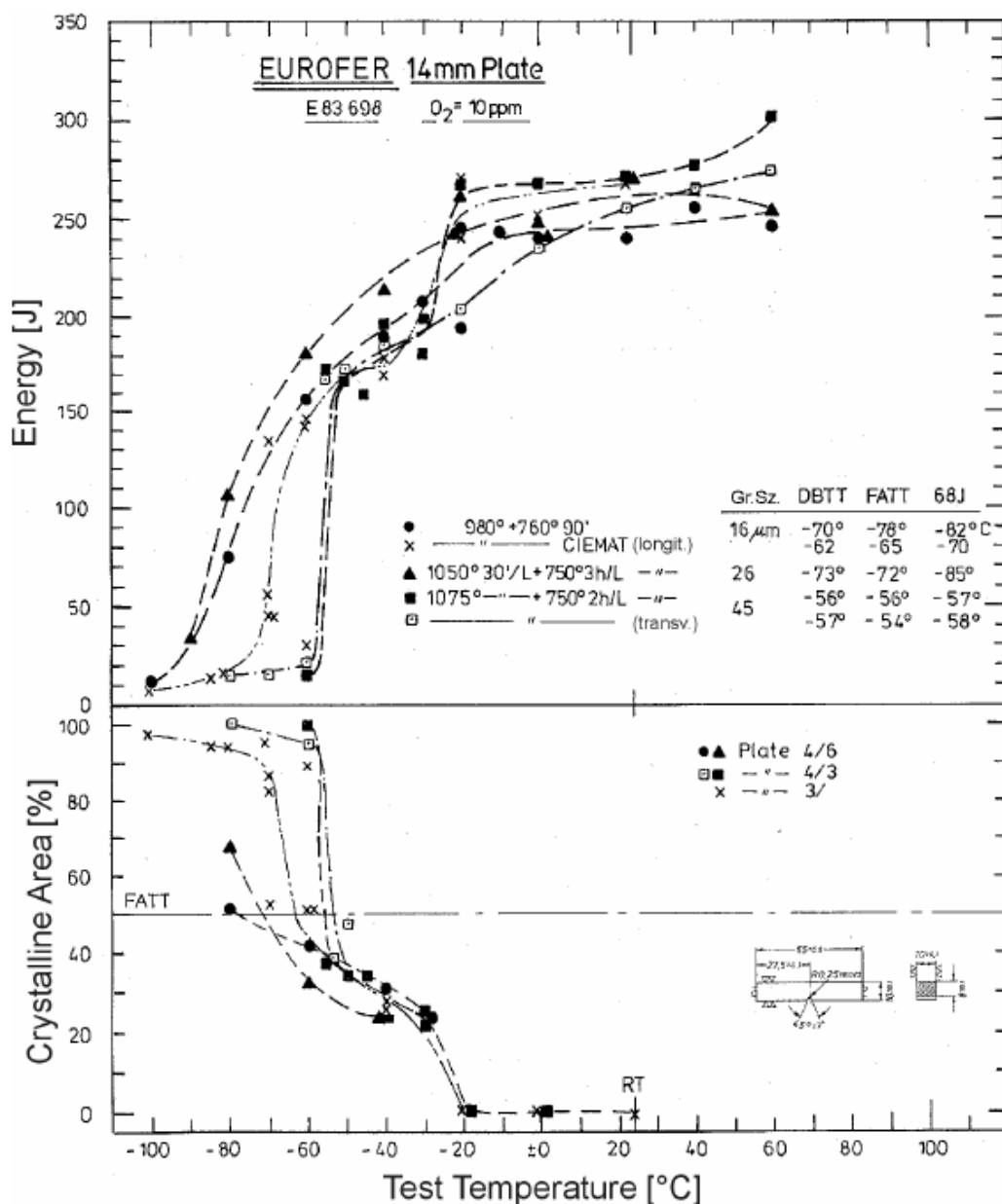


Fig.3 – Absorbed energy 8Charpy V-notch) as a function of test temperature . As can be seen, the best behaviour in term of toughness is obtained by the alloy treated at 980°Cx 1h +760àCX90'. Note as the FACT 50 increase with the increasing grain size.

On the contrary, creep tests indicates that the creep strength increase with the austenizing temperature

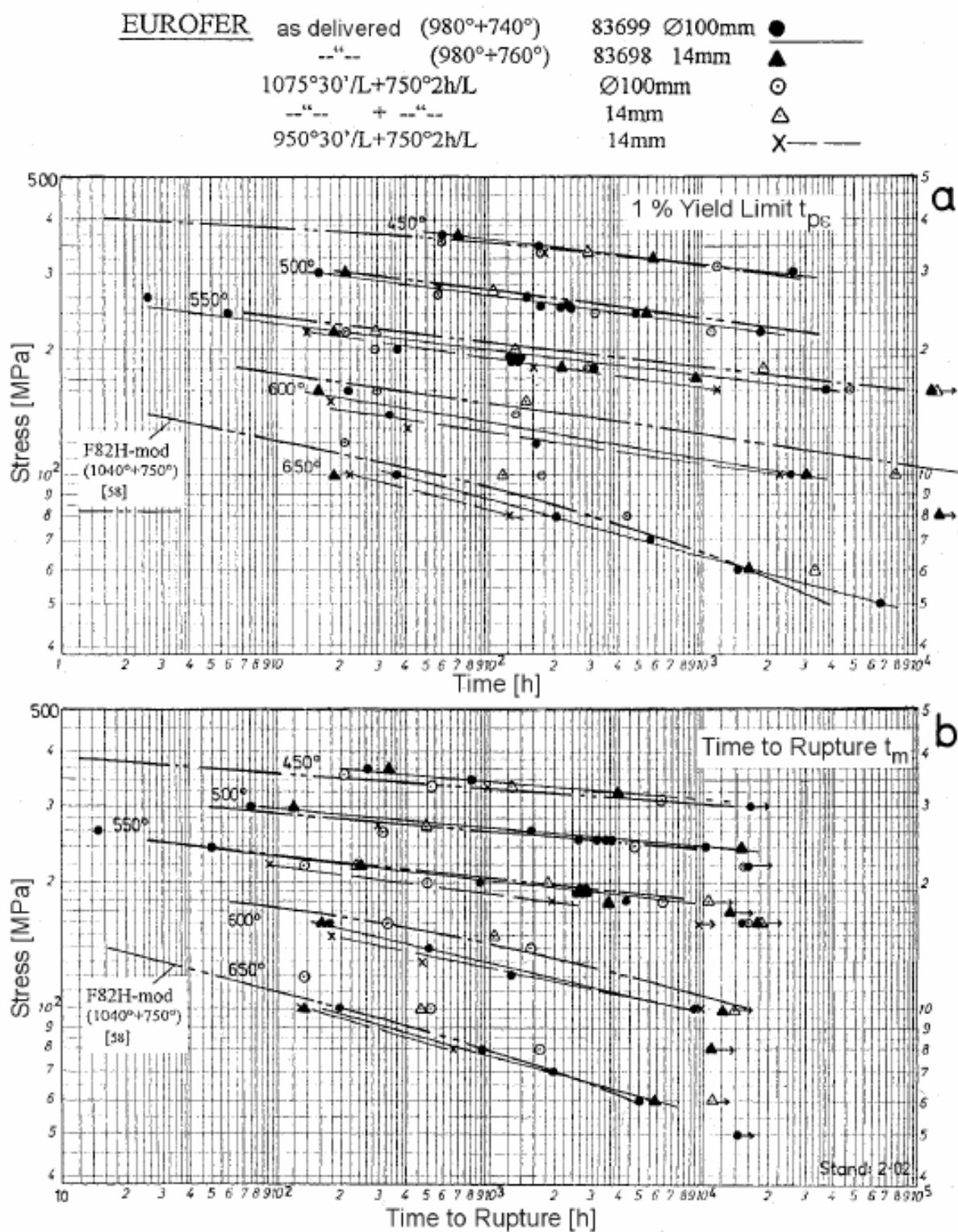


Fig.4 Creep strength of EUROFER 97 as the function of heat treatments

Despite this optimized behaviour concerning mechanical out of pile mechanical behaviour, the after irradiation exhibit several problem for temperatures lower than 380°C.

In the following figure[2] the after irradiation fracture toughness behaviour is reported while the table 3 reports the thermal treatments of irradiated alloys[2]

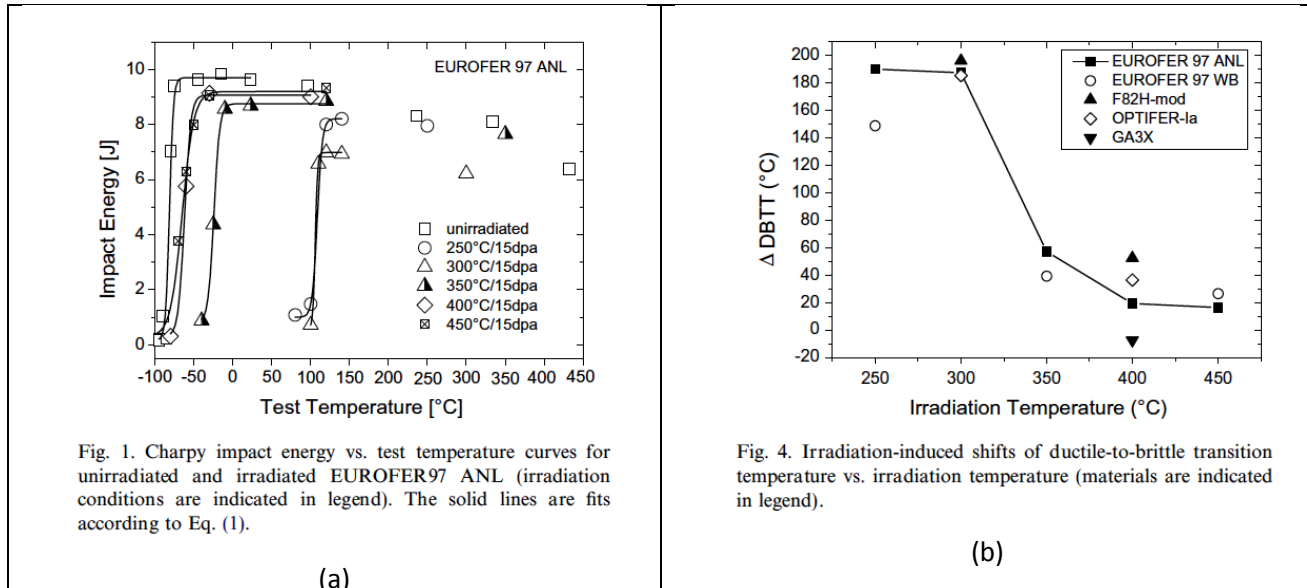


Fig.5 (a)KLST charpy impact energy versus test temperature for sample irradiated at 15 dpa; (b) DBTT shift as a function of test temperature

Table 3 Heat treatments and properties of irradiated alloys[2]

Table 2
Heat treatment and selected properties of unirradiated materials

	Heat treatment	Grain size (μm)	USE (J)	DBTT ($^{\circ}\text{C}$)	Dynamic yield stress (MPa)
EUROFER97 ANL	980 $^{\circ}\text{C}/0.5 \text{ h} + 760 \text{ }^{\circ}\text{C}/1.5 \text{ h}$	16 [5]	9.84	-81	543 @100 $^{\circ}\text{C}$
EUROFER97 WB	1040 $^{\circ}\text{C}/0.5 \text{ h} + 760 \text{ }^{\circ}\text{C}/1.5 \text{ h}$	21.4 [5]	9.84	-91	486 @100 $^{\circ}\text{C}$
GA3X	1000 $^{\circ}\text{C}/1 \text{ h} + 700 \text{ }^{\circ}\text{C}/2\text{h}$	55 \pm 5	9.4	-58	650 @100 $^{\circ}\text{C}$
F82H-mod	950 $^{\circ}\text{C}/0.5\text{h} + 750 \text{ }^{\circ}\text{C}/2\text{h}$	55	9.7	-86	446 @100 $^{\circ}\text{C}$
OPTIFER-Ia	900 $^{\circ}\text{C}/0.5\text{h} + 780 \text{ }^{\circ}\text{C}/2\text{h}$	10	10.6	-81	482 @23 $^{\circ}\text{C}$
MANET-I	980 $^{\circ}\text{C}/2\text{h} + 1075 \text{ }^{\circ}\text{C}/$ $0.5\text{h} + 750 \text{ }^{\circ}\text{C}/2\text{h}$	30 \pm 5	6.6	-30	670 @100 $^{\circ}\text{C}$

As can be seen from the experimental data the best behaviour, from the point of view of toughness, in the EUROFER 97 version WB. This alloy differs from the ANL one for the heat treatment. The ANL version, namely the standard version of EUROFER, is austenitized at 980°Cx30' and tempered at 760°Cx 1.5h, exhibiting a grain size of 16 μm , while the WB version is austenitized at 1040°C, tempered at the same temperature and time and exhibit a slightly higher grain size (21.4 μm). Taking into account that the error in the calculation of DBTT could be valuates as 10%, we can deduce that, despite the ANL and WB version have the same toughness behaviour before irradiation, after irradiation the alloy austenitized at a higher temperature exhibits a better behaviour. The same consideration could be done for the 9Cr2WVT ORNL, whose composition is reported in table [3]

Tab.4 Chemical composition of 9Cr2WVTa[4]

Steel	C	Si	Mn	Cr	Ni	Mo	W	V	Nb	B	N	Other
ORNL 9Cr-2WVTa	0.10	0.30	0.40	9.0			2.0	0.25			0.025	0.07 Ta

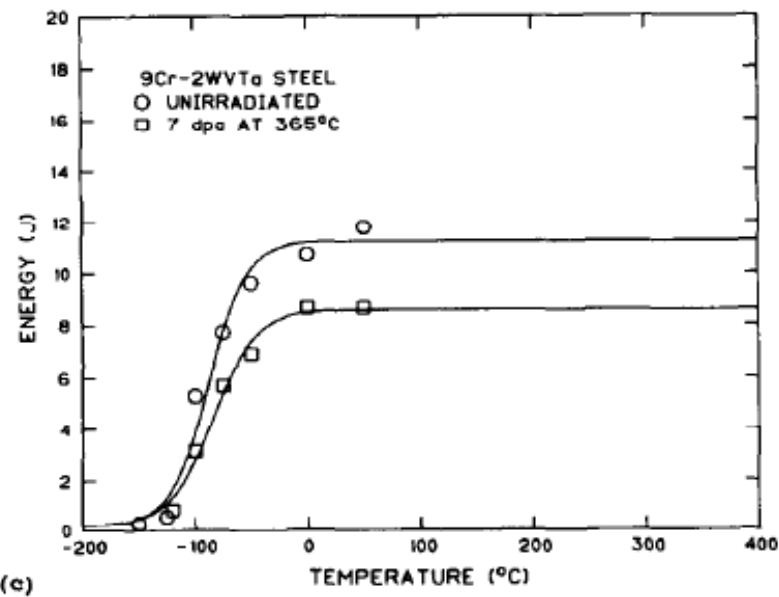


Fig. 6 – Impact behaviour of ORNL 9Cr2WVTa austenitized at 1050°Cx1h and tempered at 750°C x 1 h [4]

The low temperature embrittling phenomenon is common to all the martensitic alloy tested and goes to saturation for a damage greater than 20 dpa[5] (Fig. 6)[5]

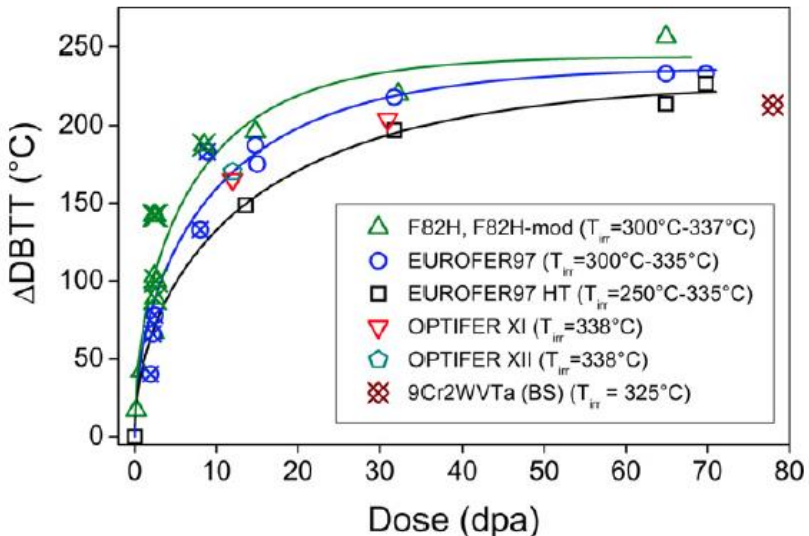


Fig. 6. Irradiation shifts of the DBTT vs. dose for EUROFER97 and other RAFM steels. The open symbols represent KIT results [3,7,9,11,17] and the crossed symbols are from [6,10,12]. The solid lines are a model description of the data [3].

The experimental results indicates that not only the grain size controls the fracture toughness but, after irradiation, it is important that the primary precipitation that controls the grain size would be fine. In effect, although the normalizing treatment at 980°Cx0.5 give a very fine grain size (about 16 μm) and the alloy exhibit the best before irradiation behaviour, after irradiation the best results are obtained from those alloy that were austenitized at higher temperature (about 1040-1050°C). When the austenitizing temperature is very low, the grain size is very fine but the volumetric fraction of primary precipitation (e.g, TaC) in high and their dimensions are also relevant. When the austenitizing temperature increase the volumetric fraction on primary precipitation decrease and decrease also the mean dimension. So it would be important to have, at

the same time The finest grain size and the finest primary precipitation. This effect can be obtained performing multiple austenitization treatments[7][8] at temperatures greater than the minimum austenitization temperature . One of the aim of this investigation will be to find the temperature and the number of austenitizing treatment to perform before tempering to minimize the grain size.

These experimental facts and the consideration that can be deduced bring us to define our development lines as follows:

- To Reduce of Nitrogen content to have a slightly soft matrix and to reduce secondary precipitation at the tempering temperature (VTan)
- To reduce the Vanadium amount for the same reasons.
- To keep the Ta and Carbon concentrations at the same value of Eurofer to have the primary precipitation required to refine the grain size.
- To study the effect of multi-austenitization treatments before tempering in order to have at the same time small grain size and finer primary precipitation of TaC and to fix, after investigations, the normalizing and tempering treatment.

These consideration will be sustained by thermo-dynamical considerations that will be described in the following sections.

The other items to be examined is the Cr effect on embrittling phenomena. It is well known the formation of α' phase for spinodal decomposition for martensitic alloys with a Cr content in the order of 12%[9]. These small Cr-rich ferrite harden the matrix and contribute to embrittle the irradiated martensite at temperature greater than 400°C. This brought to develop martensitic 9Cr alloy for Fast Breeder Reactor applications (e.g. Grade 91 and EM10).

The literature seems to show that the Cr amount that minimize the DBTT shift would be about 9% [9], as reported in the following figure.

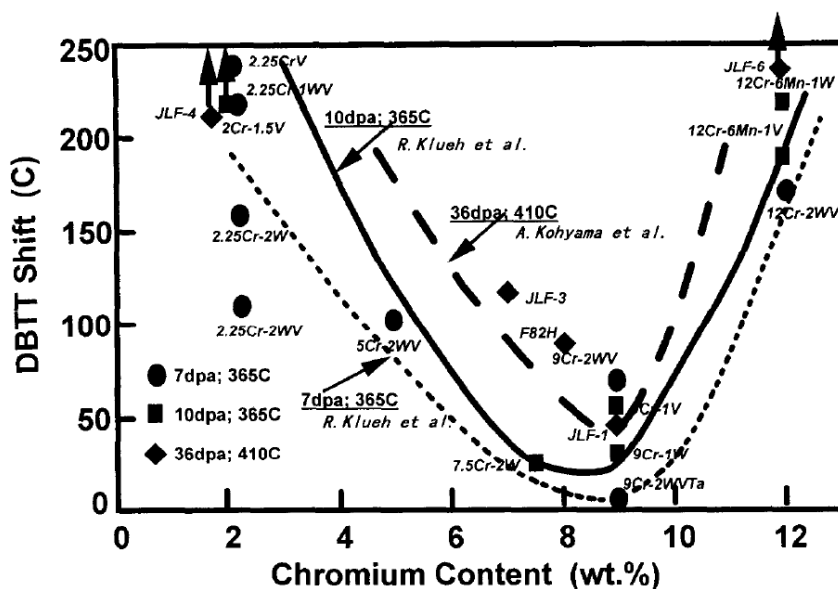


Fig. 3. Effect of chromium content on DBTT shift of LAFs by neutron irradiation in FFTF.

Fig.7 – General overview of the Cr content versus the DBTT shift[9]

It is our opinion that this comparison is too much generic because there are comparison between several different alloys, not only for the Cr content but also for other elements, and the microstructure are not optimized to reduce the under irradiation embrittlement. In fact, recent experimentation on model Fe-5Cr alloys exhibits Cr segregations on interstitial loops created under irradiations[10]

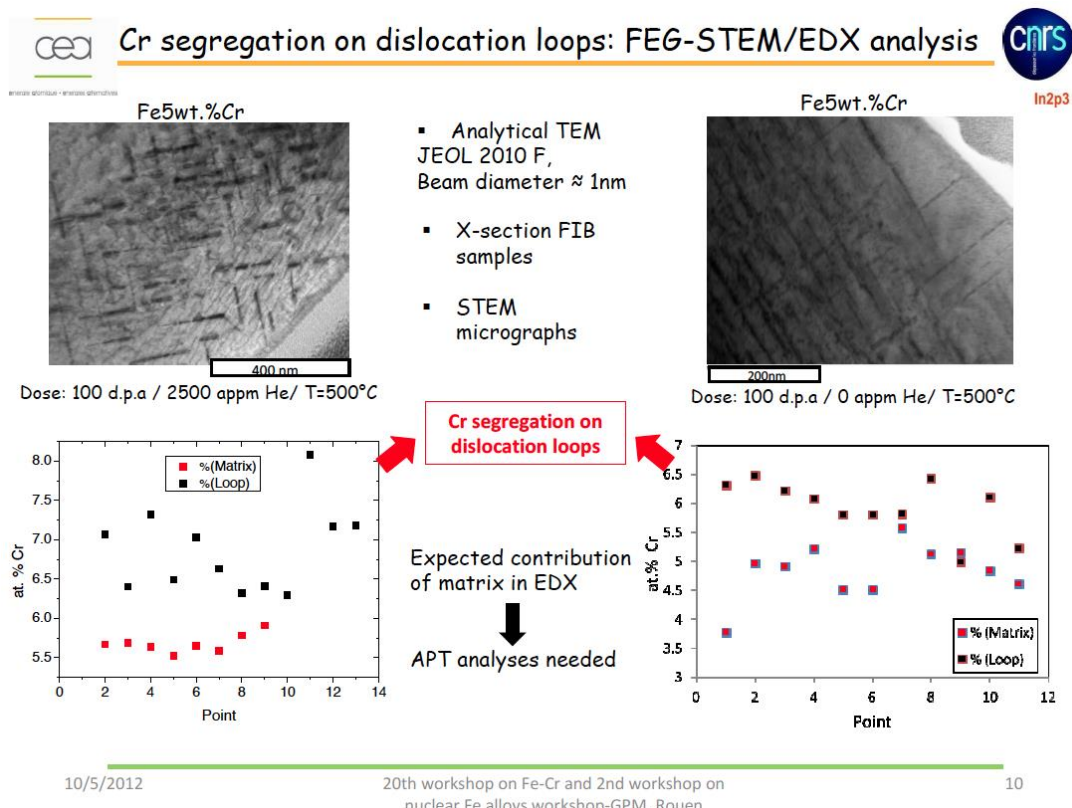


Fig.8 – Irradiated Fe-5Cr model alloys in JANUS and examined with a FEG-STEM+EDX that show the Chromium enrichment in correspondence of dislocation loops created by irradiations[10].

The Chromium segregation on dislocation loops could stabilize the loops against dissolution or intersections with other loops if the segregated chromium should tend to decrease the stacking fault energy. The decreasing of stacking energy enlarges the defects and reduces the probability of climbing and recombinations with opposite defects. This Cr segregation should be likely dependent on the Cr concentration, namely the greater the Chromium concentration the greater will be the Chromium concentration within the interstitial loop bringing to the α' formation for Chromium level very high. These considerations justify experimenting the behaviour of a RAFM with a lower level of Chromium, similar, in any case, to the international cast F82H, although the rest of the chemistry and the thermal treatments will be different. In conclusion:

- We want To Reduce the chromium amount compatibly with corrosion behaviour and in the range of RAFM just studied (e.g. F82H);

All these considerations were developed because The recent EUROFUSION requirements indicate that the first DEMO reactor will be water-cooled. This implies that the minimum irradiation temperature would be about 280°C. So, in the WP-MAT, in light of the under irradiation behaviour of EUROFER and the consideration exposed before, it was decided to develop a much tough alloy, able to tolerate the so low irradiation temperature with a slightly Chromium content compared with the amount of EUROFER.

2 DESCRIPTION OF ACTIVITIES AND RESULTS

2.1 THERMODYNAMIC SIMULATIONS

The activities carried out in this period consisted in thermodynamic simulations performed with the code THERMOCALC with database TCFE7. We analized the thermodynamic of phases of true eurofer 97 and compared those results with new theoretical composition with the aim to maintain a certain amount of primary precipitation to control and minimize the grain size and, at the same time, to have an alloy less resistant to the temper, namely a matrix that could be softened at level slightly higher than eurofer. This In the following we report the thermodynamic graphs of the field of existence of the stable phases

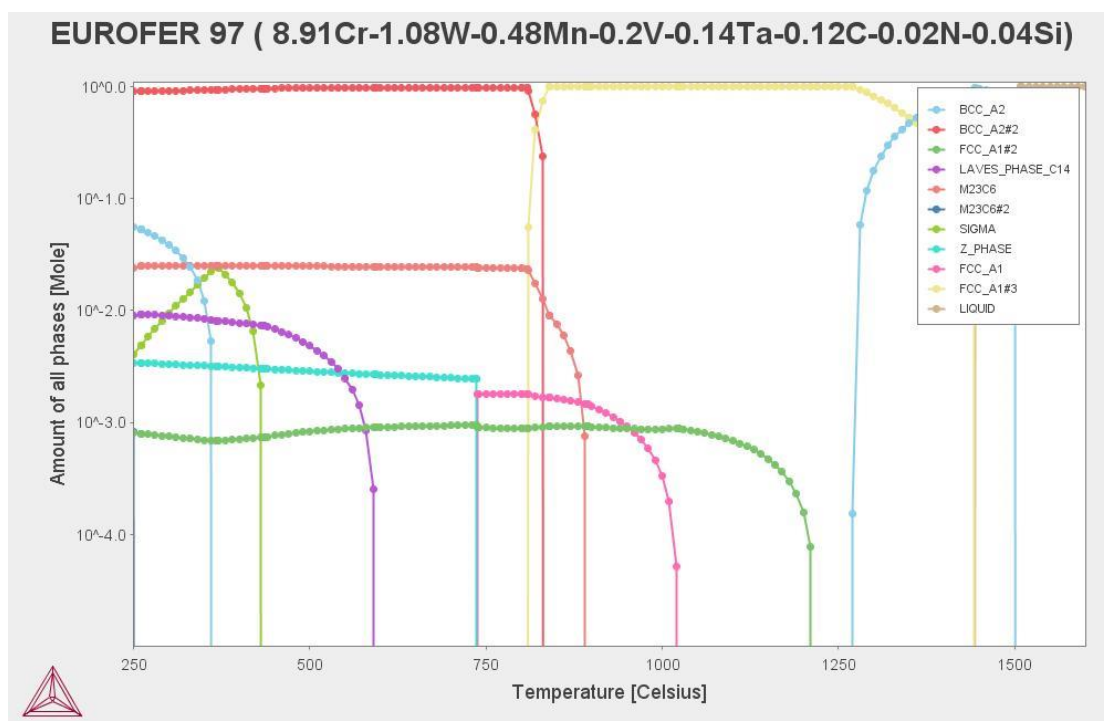


FIG.8 Phase stability diagram of EUROFER

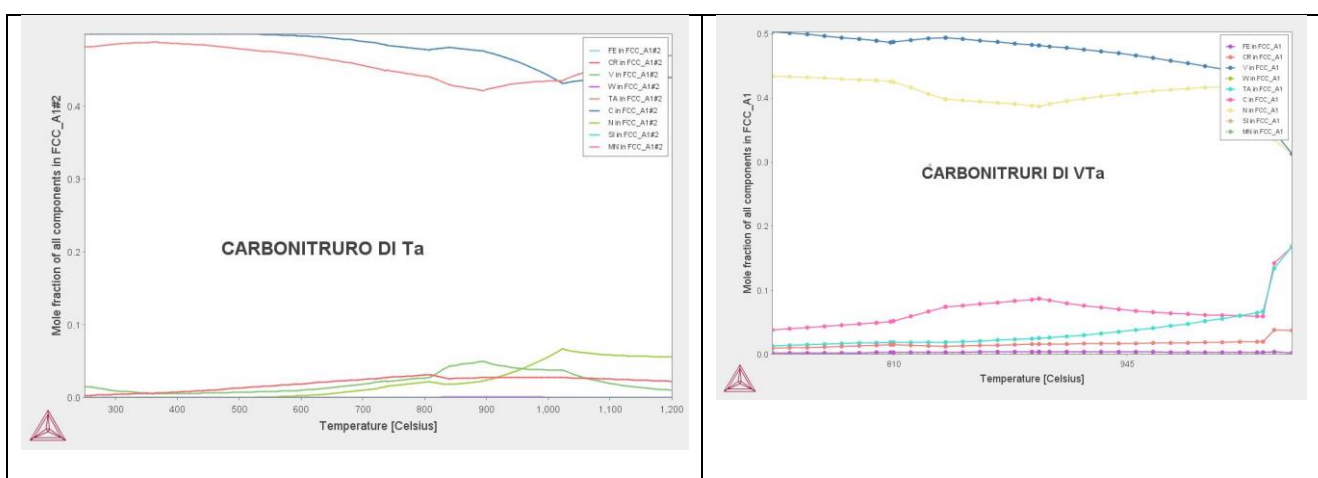


Fig 9. Chemical compositions of Primary Carbides (TaC) and secondary carbides (VCN) EUROFER 97

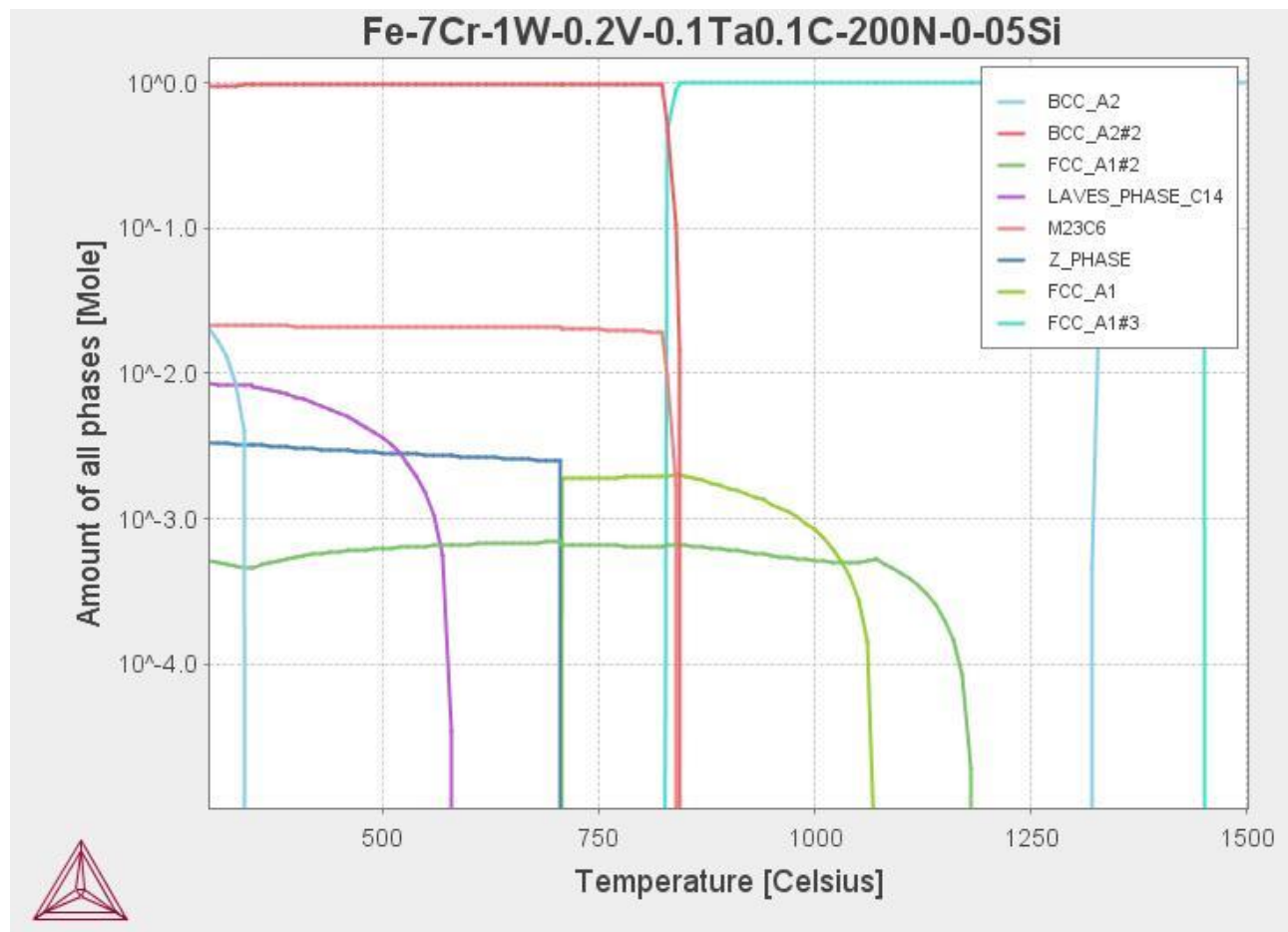


FIG.10 Phase stability diagram of Fe-7Cr-1W-0.2V-0.1Ta-0.1C-0.5Mn-0.05Si

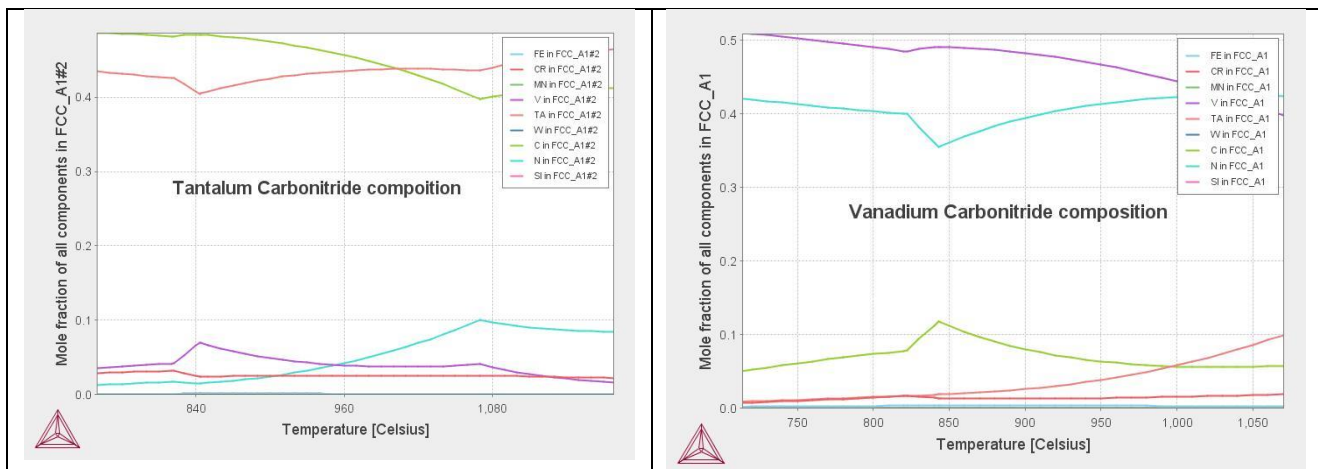


Fig11. Chemical compositions of Primary Carbides (TaC) and secondary carbides (VCN)

2014.09.19.16.00.52

TCFE7: Fe, Cr, V, Ta, W, C, N, Si

Pressure [Pascal] = 1000000.0, System size [Mole] = 1.0, Mass percent Cr = 7.0, Mass percent V = 0.2, Mass percent Ta = 0.1, Mass percent W = 1.0, Mass percent C = 0.1, Mass percent N = 0.007, Mass percent Si = 0.05

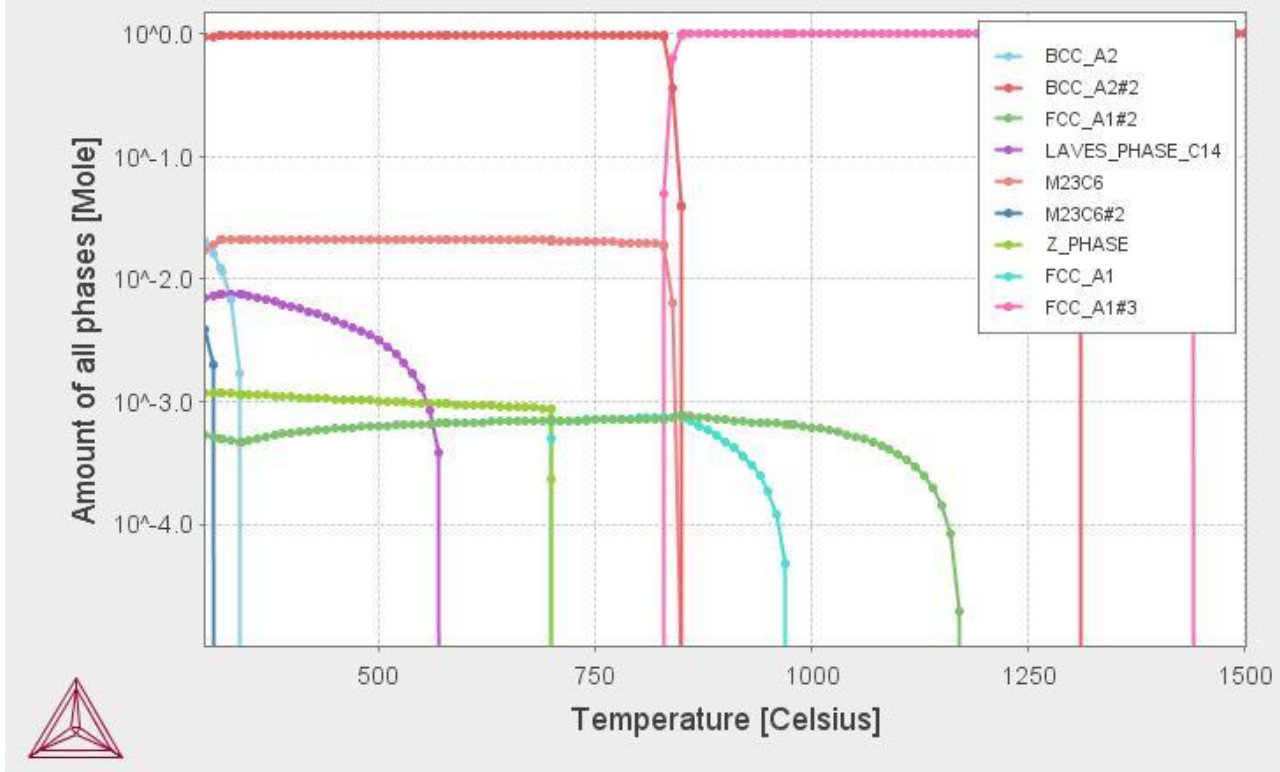


Fig.12 Phase stability diagram of Fe-7Cr-1W-0.2V-0.1Ta-0.1C-0.05Si-0.007N

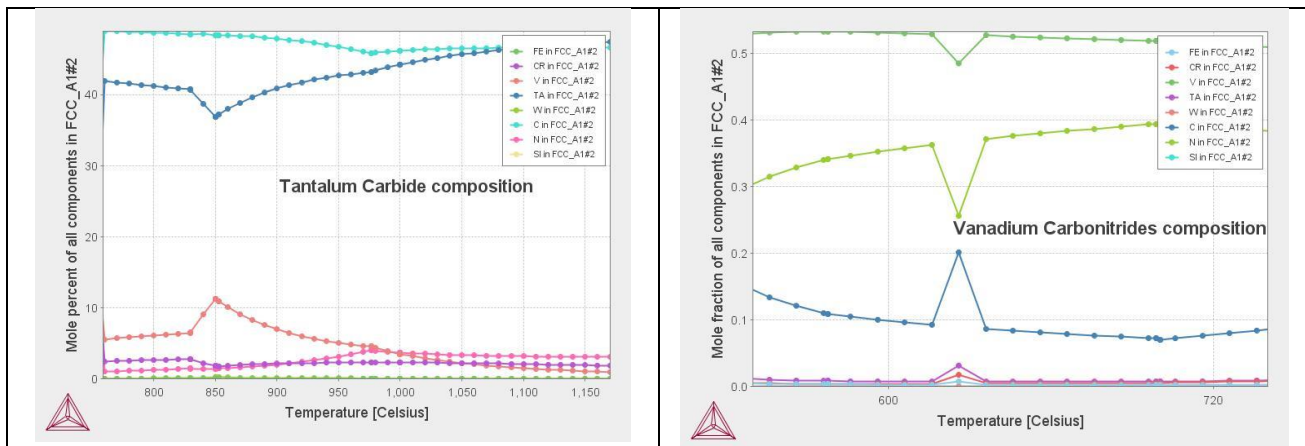


Fig13. Chemical compositions of Primary Carbides (TaC) and secondary carbides (VCN)

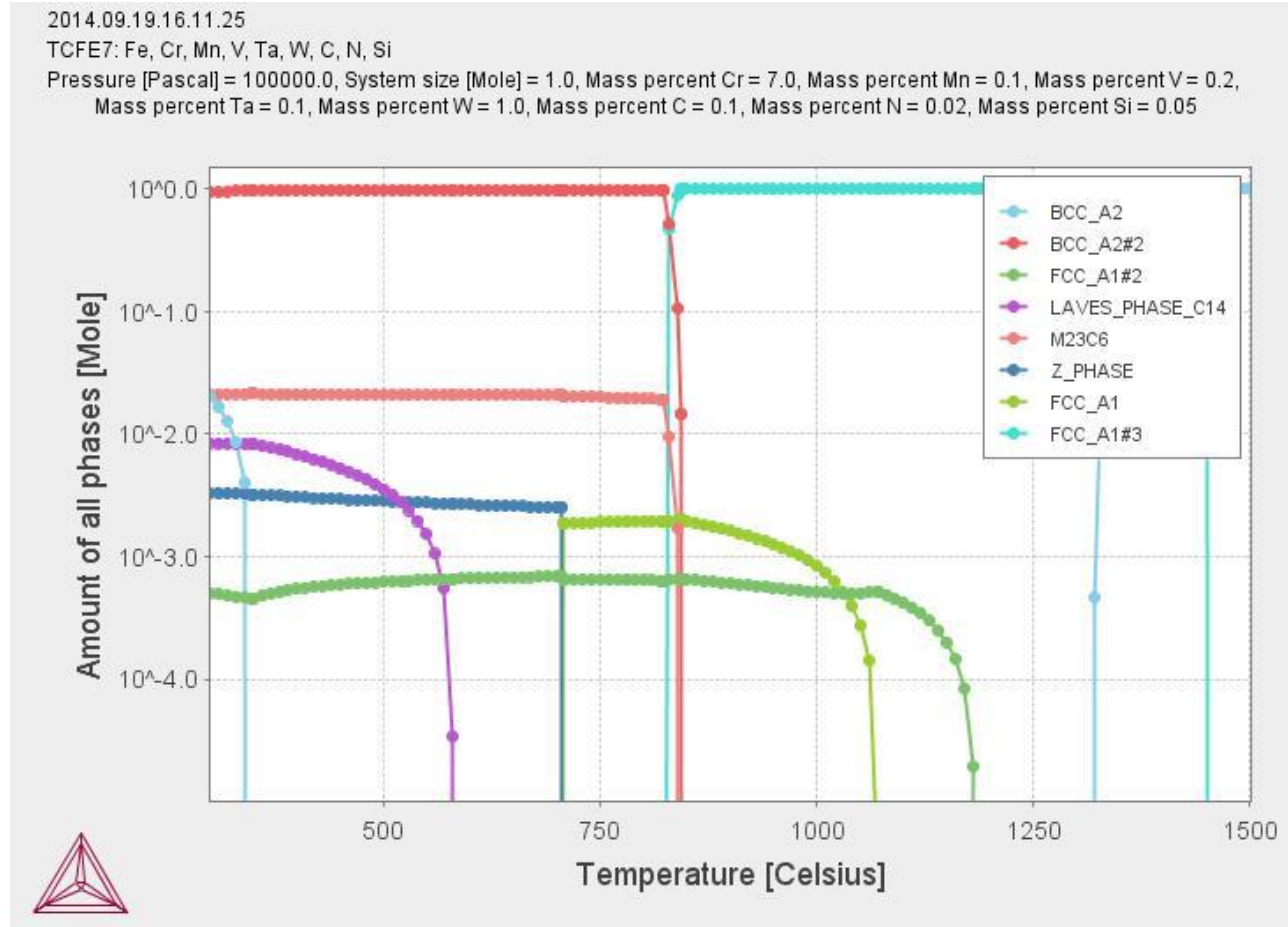


Fig.14 Phase stability diagram of Fe-7Cr-1W-0.2V-0.1Ta-0.1C--0.05Si-0.02N-0.1Mn

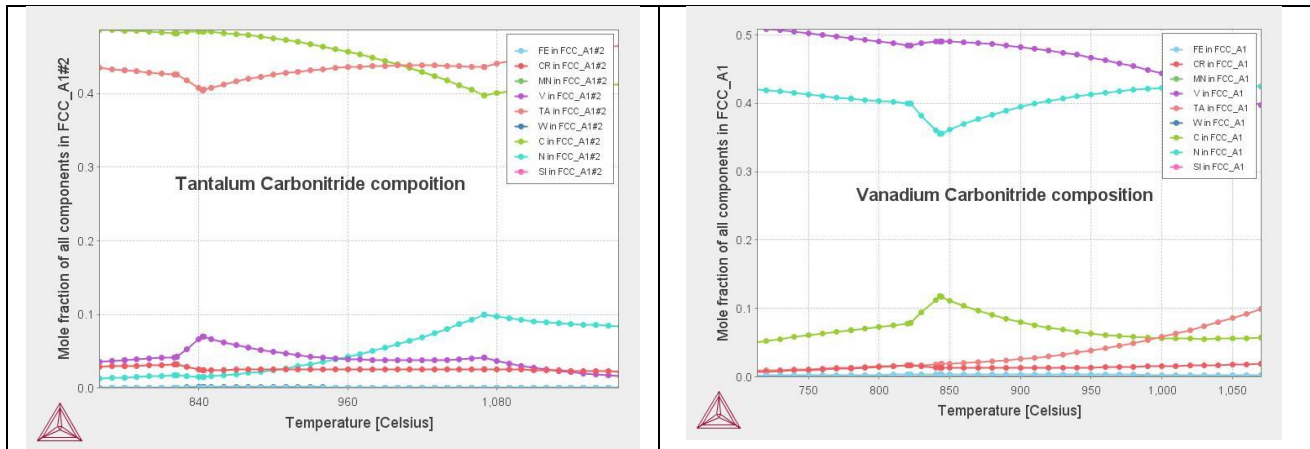


Fig.15. Chemical compositions of Primary Carbides (TaC) and secondary carbides (VCN)

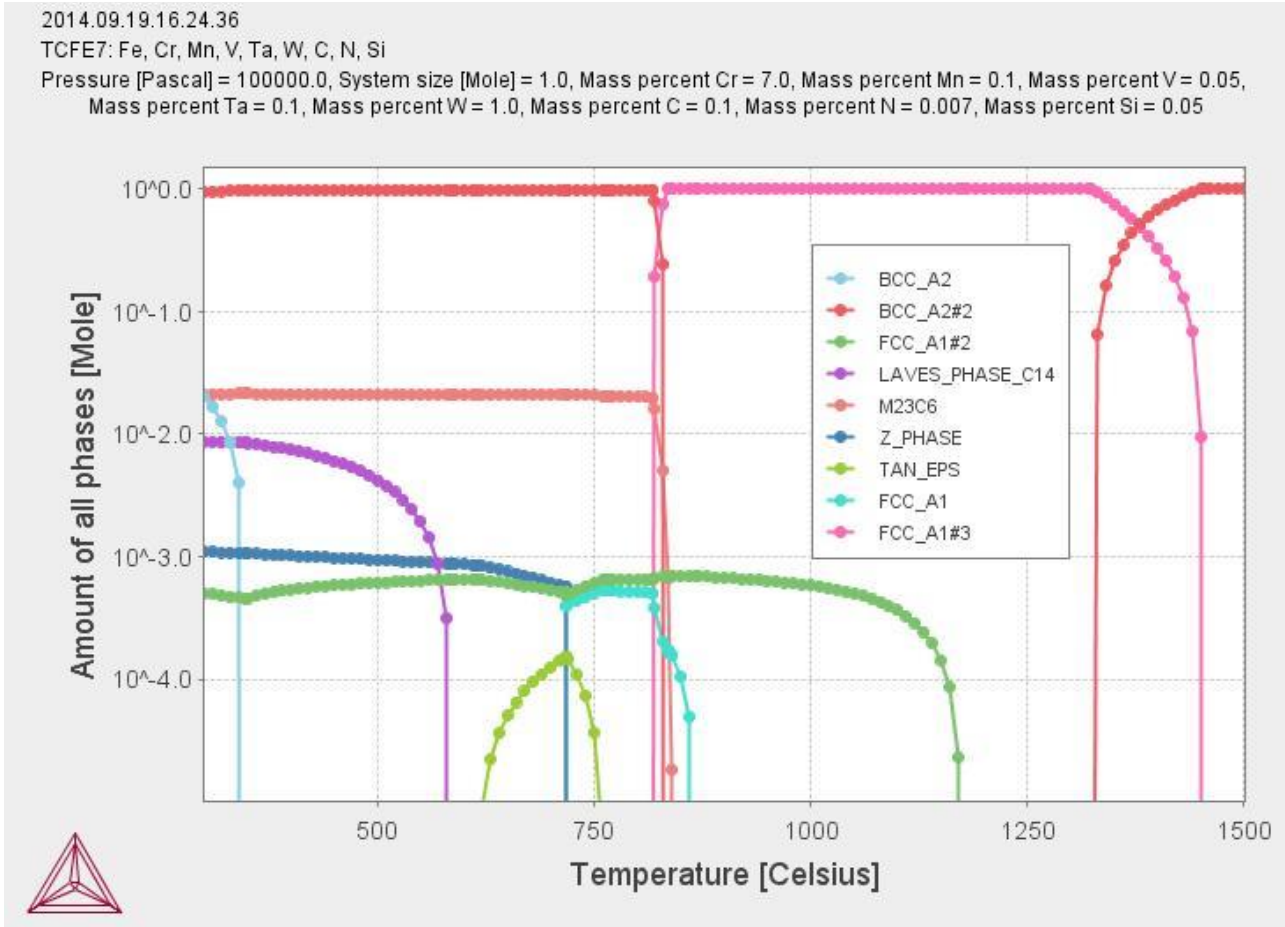


Fig.16 Phase stability diagram of Fe-7Cr-1W-0.05V-0.1Ta-0.1C--0.05Si-0.007N-0.1Mn

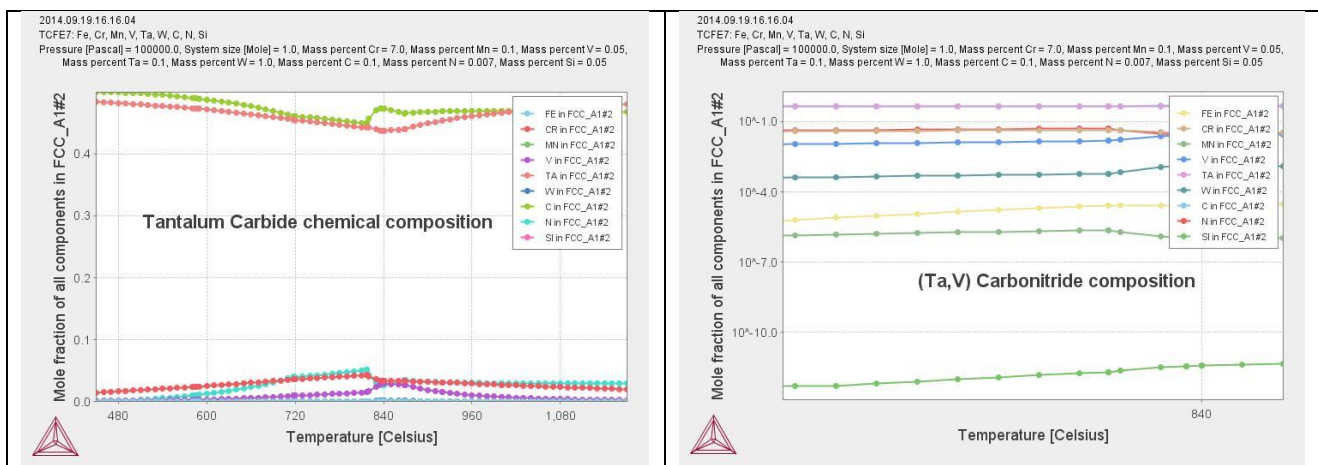


Fig17. Chemical compositions of Primary Carbides (TaC) and secondary carbides (Ta,V)(C,N)

On the basis of these calculation, having verified that the total amount of secondary precipitation, responsible on tempering resistance, was lowered of about 20% respect to EUROFER97 and having conserved at the same time a primary precipitation needed to control the grain size, we have fixed the specifications that, together with the preliminary analysis of the ingot produced by CSM, satisfy these requirement. The specifications and the preliminary analysis are reported in Table 4.

Tab. 4- Preliminary chemical analysis of the ingot produced by CSM

Bollettino di prova

	codice	nome
Laboratorio	72	U.O. FABBRICAZIONE LEGHE e PROTOTIPIAZIONE
Tipo di prova	72018	FABBRICAZIONE LINGOTTO BASE Fe 80 kg
n° colata	VM2886	n° commessa RD010132
Acciaio/lega	7Cr	

COMPOSIZIONE CHIMICA [%]																
	Fe	Ni	Cu	Cr	W	Mo	Nb	Al	Ti	Si	Mn	P	C	S	O	N
min	bal			6,80	1,00					0,030	0,09		0,080			
max	bal			7,20	1,20					0,050	0,11		0,120			
aim	bal	<0,02	<0,01	7,00	1,00	<0,01	<0,01	<0,01	<0,01	0,040	0,10	<0,006	0,100	<0,005	<0,004	<0,01
real	bal	<0,02	<0,01	7,05	1,00					0,045	0,11		0,091	0,0015		0,0026

	Co	Ta	V	Ce	Y	B	Ca	Hf	La	Zr	Zn	Bi	Pb	Sn	Sb	As
min		0,05														
max		0,11														
aim	<0,01	0,10	<0,05	<0,005		<0,001				<0,005				<0,005	<0,005	<0,005
real		0,10														

Data: 17 settembre 2014

Eseguita da: Cialfi/Marani

Responsabile di laboratorio: R. Sorci

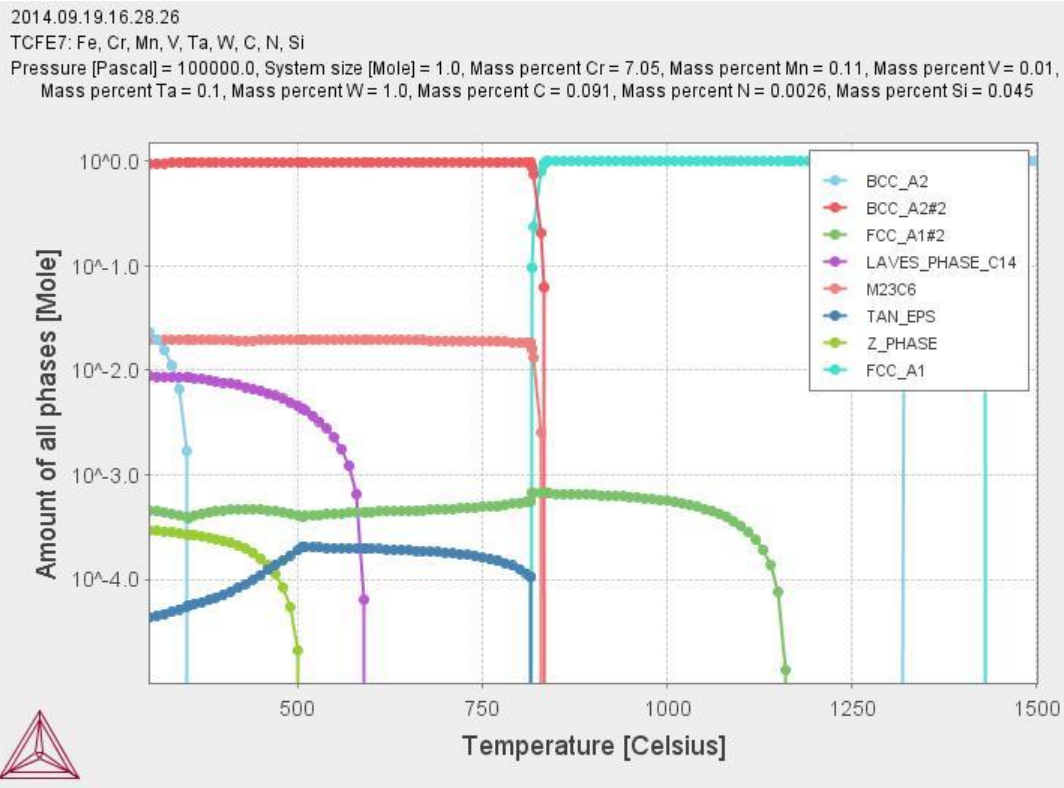


Fig.18 Phase stability diagram of Fe-7Cr-1W-0.05V-0.1Ta-0.1C-0.05Si-0.007N-0.1Mn

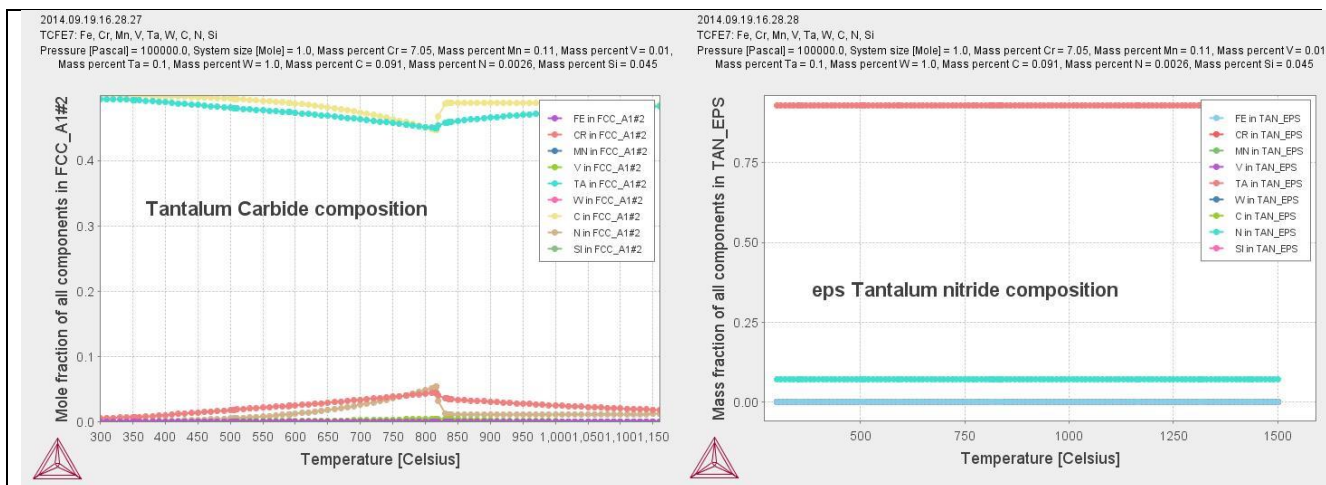


Fig19. Chemical compositions of Primary Carbides (TaC) and secondary carbides eps -TaN

In the following table we have resumed the major properties.

Tab.5 Properties of alloys studied in this work

EUROFER97	int 100%γ	M23C6	fM23C6	TaC	fmax TaC	VCN	fmax VCN	zph	maxr2phase	TaN eps	ffTaN eps	Laves	Sigma	alfa'	Ae1	Ae3	delta	TOTAL MOLAR FRACTION OF PRECIPITATES
EUROFER97	837-1267	891	0.0248	1212	0.00091	1016	0.0018	737	0.002			591	432	366	810	837	1269	0.02951
7Cr1W0.1Ta0.1CI	830-1326	840	0.0197	1179	0.00062	1059	0.0024	707	0.0033			580	411	340	809	830	1329	0.02602
7Cr1W0.1Ta0.1CI	844-1319	844	0.0204	1179	0.000633	1066	0.002	706	0.0033			576	0	340	830	844	1320	0.026333
7Cr1W0.1Ta0.1CI	852-1307	849	0.0288	1172	0.00079	970	0.00076	698	0.00121			573	0	340	839	852	1310	0.03156
7Cr1W0.1Ta0.1CI	841-1321	840	0.0213	1173	0.00073		0.00065	717	0.0008			580	0	340	817	840	1323	0.02348
7Cr colata CSM	837-1314	833	0.0197	1161	0.00067		0.00029	814	0.000194	589	0	346	818	837	1314		0.020854	

The value reported in the table are the following:

- 100% austenite field, initial precipitation of various phase and relative molar fractions, Ae1, Ae3, the lower temperature of formation of delta ferrite and the total molar fraction amount of precipitates. From the table result that the total amount of molar fraction of precipitates of EUROFER 97 is about 2.95% amount while in the CSM cast this value is about 2.08%, with a 30% of reduction of total precipitation, as desired.

2.2 FABBRICATION

In what follows we report the CSM report of the cast fabrication. The preliminary analysis was just seen in table 4.

2.3 Fabbricazione lingotto 7Cr (mini report CSM)

Il lingotto 7Cr (fig.1) è stato realizzato all'interno del laboratorio "Tecnologie Fusorie & Chimica Metallurgica", mediante la tecnologia fusoria in vuoto VIM (Vacuum Induction Melting), che è il processo di fusione più versatile per la produzione di quasi tutte le leghe speciali base Fe, Ni e Co.

L'impianto VIM del CSM (ALD-Vacuum Technologies) (fig. 2) impiegato per la produzione dei lingotti, possiede le seguenti caratteristiche tecniche:

- Intervalli di fusione: 1300 – 1600 °C;
- Atmosfera: Vuoto/gas inerte;
- Pressione di lavoro: da 5×10^{-5} mbar a 300 mbar;
- Range di misura temperature: da 750 a 1800°C (tramite termocoppie e pirometri ottici);
- Colaggio: Lingottiera/Guscio ceramico;
- Volume di fusione/colaggio: da 1 a 11 dm³;



Fig. 1 – Lingotto 7Cr



Fig. 2 – Impianto VIM (ALD-Vacuum Technologies) presso il CSM

Il processo di fusione della carica avviene tramite una bobina di rame, raffreddata ad acqua, attraverso la quale passa una corrente alternata che avvolge il crogiolo di refrattario generando così delle correnti parassite nel materiale di carica che si scalda per effetto joule.

L'agitazione ('stirring magnetico') che il processo genera nel bagno garantisce sia la omogeneizzazione e il controllo più accurato della chimica e della temperatura del fuso, sia il trasporto di materia necessario per lo svolgimento delle reazioni chimico-fisiche richieste, come per esempio, il degasaggio.

Tale processo garantisce inoltre un'esatta composizione e riproducibilità del prodotto.

Il ciclo di fusorio in un forno VIM è strutturato in diversi passaggi: carica, fusione, affinazione, analisi chimica e correzione della composizione, colaggio.

Il materiale di carica è comprensivo degli elementi leganti, eccetto i costituenti reattivi, che vengono introdotti successivamente mediante un sistema di carica posto sulla sommità del forno. Durante la fusione e l'affinazione avvengono reazioni quali il degasaggio e la disossidazione.

Alla fine del periodo di affinazione vengono introdotti, se necessari, gli elementi reattivi quali Si e Mn.

Dopo un tempo richiesto per il mescolamento ottimale del bagno si procede ad un'analisi chimica ed ad eventuali aggiunte di alliganti nel caso di carenze nella composizione. Alla fine il fuso viene colato in lingottiera.

In questo caso per i materiali di carica sono state utilizzate materie prime con purezza non inferiore al 99.9%.

Sono stati prodotti n°1 lingotto, di dimensioni 200x100 mm e altezza 400mm per un totale di circa 40kg di materiale.

Il ciclo fusorio seguito è mostrato in fig. 3. Il grafico riporta l'andamento dei valori di vuoto, di potenza e di temperatura del forno ad induzione in funzione delle diverse fasi del processo.

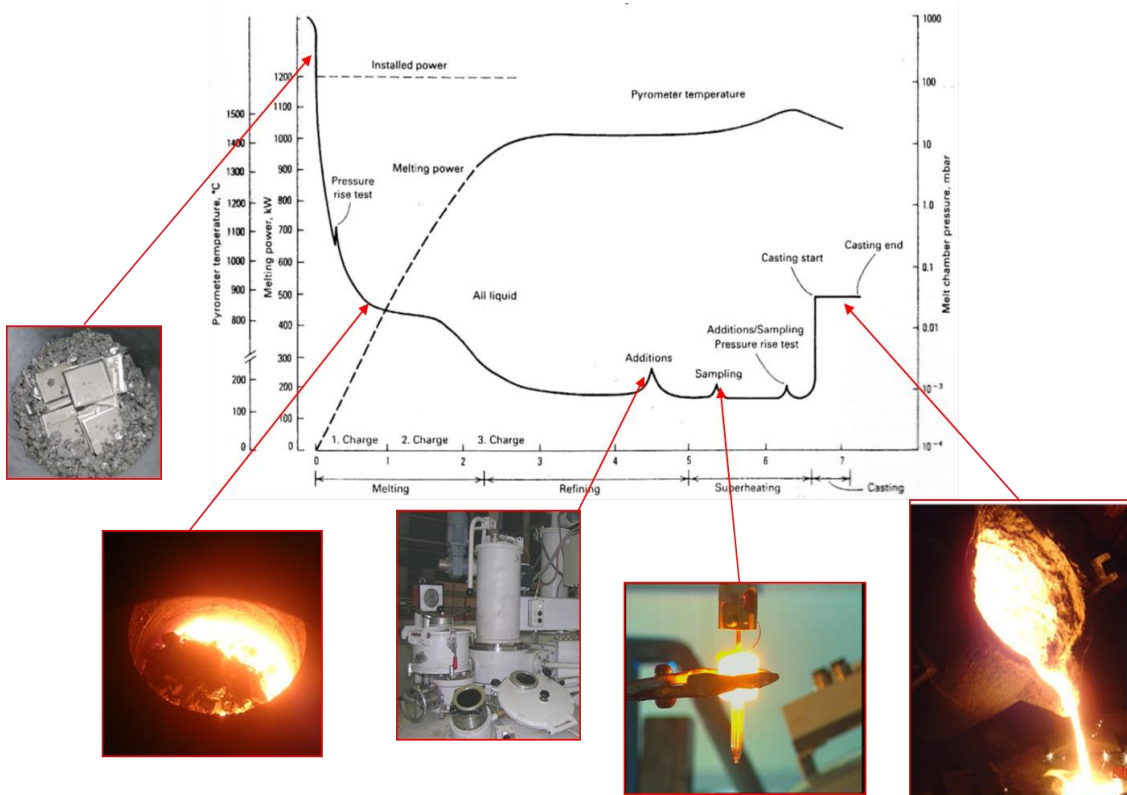


Fig. 3 - Differenti fasi del ciclo fusorio

I risultati ottenuti in termini di composizione chimica sono riportati nella tabella di seguito, in cui si evince il perfetto raggiungimento dei target compostizionali richiesti.

Bollettino di prova



	codice	nome
Laboratorio	72	U.O. FABBRICAZIONE LEGHE e PROTOTIPAZIONE
Tipo di prova	72018	FABBRICAZIONE LINGOTTO BASE Fe 80 kg
n° colata	VM2886	n° commessa RD010132
Acciaio/lega	7Cr	

COMPOSIZIONE CHIMICA [%]																
	Fe	Ni	Cu	Cr	W	Mo	Nb	Al	Ti	Si	Mn	P	C	S	O	N
min	bal			6,80	1,00					0,030	0,09		0,080			
max	bal			7,20	1,20					0,050	0,11		0,120			
aim	bal	<0,02	<0,01	7,00	1,00	<0,01	<0,01	<0,01	<0,01	0,040	0,10	<0,006	0,100	<0,005	<0,004	
real	bal	<0,02	<0,01	7,05	1,00					0,045	0,11		0,091	0,0015	0,0026	

	Co	Ta	V	Ce	Y	B	Ca	Hf	La	Zr	Zn	Bi	Pb	Sn	Sb	As
min		0,05														
max		0,11														
aim	<0,01	0,10	<0,05	<0,005		<0,001				<0,005			<0,005	<0,005	<0,005	<0,005
real		0,10														

Data: 17 settembre 2014 Eseguita da: Cialfi/Marani Responsabile di laboratorio: R. Sorci

Specifica richiesta

Fig. 4 – composizioni chimiche lega madre

3 Conclusioni

The activities performed in these framework, based on the theoretical study of martensitic alloy characteristic of a FUSION environment, with the aim to reach the goal to have a much more toughen alloy after irradiation at temperature so low as 280°C, allowed us to define and fabricate a promising alloy that will be tested in the prosecution of the programme.

4 Riferimenti bibliografici

- [1] M.Rieth,M.Shirra, A.Falkenstein,P.Graf,S.Heger,H.Kempe, R.Lindau, H Zimmerman Wisenschaftliche Berichte FZKA 6911
- [3] R.L Klueh : *Ferritic/martensitic steels for advanced nuclear* Transactions of The Indian Institute of MetalsVol. 62, Issue 2, April 2009, pp. 81-87
- [4] R.L. Klueh, D.J. Alexander and P.J. Maziasz. *Impact behavior of reduced-activation ferritic steels irradiated in the Fast Flux Test Facility*. Journal of Nuclear Materials 186 (1992) 185-195
- [5] E.Gaganidze, J.Aktaa Fusion Engineering and Design
- [6] John William MORRIS, Jr. *On the Ductile-Brittle Transition in Lath Martensitic Steel* ISIJ International,

Vol. 51 (2011), No. 10, pp. 1569–1575

- [7] Pilloni, L., Attura, F., Calza-Bini, A., De Santis, G., Filacchioni, G., Carosi, A., Amato, S. *Physical metallurgy of BATMAN II Ti-bearing martensitic steels* (1998) Journal of Nuclear Materials, 258-263 (PART 2 B), pp. 1329-1335
- [8] Chunfang Wang, Maoqiu Wang, Jie Shi, Weijun Hui and Han Dong *Effect of microstructural refinement on the toughness of lowcarbon martensitic steel*. Scripta Materialia 58 (2008) 492–495
- [9] A. Kohyama a, A. Hishinuma b, D.S. Gelles , R.L. Klueh d, W. Dietz , K. Ehrlich *Low-activation ferritic and martensitic steels for fusion application* Journal of Nuclear Materials 233-237 (1996) 138-147
- [10] A.Bhattacharya, E Meslin,B. De Camps, C. Pareige, J. Henry, A. Barbu in 20th workshop on Fe-Cr ans 2nd workshop on nuclear Fe alloy workshop-GPM Rouen, 10 Maj 2012

5 Abbreviazioni ed acronimi

RAFM – reduced activation ferritic martensitic steel

PAGs- Prior Austenite grain size

WP-MAT Work Package Materials